Computers, Materials & Continua
DOI: 10.32604/cmc.2022.028856
Article

Deer Hunting Optimization with Deep Learning Model for Lung Cancer Classification

Mahmoud Ragab[1,2,3,*], Hesham A. Abdushkour[4], Alaa F. Nahhas[5] and Wajdi H. Aljedaibi[6]

[1]Information Technology Department, Faculty of Computing and Information Technology, King Abdulaziz University, Jeddah 21589, Saudi Arabia
[2]Center of Artificial Intelligence for Precision Medicines, King Abdulaziz University, Jeddah 21589, Saudi Arabia
[3]Mathematics Department, Faculty of Science, Al-Azhar University, Naser City 11884, Cairo, Egypt
[4]Nautical Science Department, Faculty of Maritime Studies, King Abdulaziz University, Jeddah, 21589, Saudi Arabia
[5]Biochemistry Department, Faculty of Science, King Abdulaziz University, Jeddah, 21589, Saudi Arabia
[6]Computer Science Department, Faculty of Computing and Information Technology, King Abdulaziz University, Jeddah 21589, Saudi Arabia
*Corresponding Author: Mahmoud Ragab. Email: mragab@kau.edu.sa
Received: 19 February 2022; Accepted: 30 March 2022

Abstract: Lung cancer is the main cause of cancer related death owing to its destructive nature and postponed detection at advanced stages. Early recognition of lung cancer is essential to increase the survival rate of persons and it remains a crucial problem in the healthcare sector. Computer aided diagnosis (CAD) models can be designed to effectually identify and classify the existence of lung cancer using medical images. The recently developed deep learning (DL) models find a way for accurate lung nodule classification process. Therefore, this article presents a deer hunting optimization with deep convolutional neural network for lung cancer detection and classification (DHODCNN-LCC) model. The proposed DHODCNN-LCC technique initially undergoes pre-processing in two stages namely contrast enhancement and noise removal. Besides, the features extraction process on the pre-processed images takes place using the Nadam optimizer with RefineDet model. In addition, denoising stacked autoencoder (DSAE) model is employed for lung nodule classification. Finally, the deer hunting optimization algorithm (DHOA) is utilized for optimal hyper parameter tuning of the DSAE model and thereby results in improved classification performance. The experimental validation of the DHODCNN-LCC technique was implemented against benchmark dataset and the outcomes are assessed under various aspects. The experimental outcomes reported the superior outcomes of the DHODCNN-LCC technique over the recent approaches with respect to distinct measures.

Keywords: Lung cancer; image classification; computer aided diagnosis; deep learning; medical imaging; parameter optimization

1 Introduction

Medical image analysis has remarkable superiority in the fields of healthcare industry, especially in clinical examination and non-invasive treatment [1]. The attained restorative image includes computed tomography (CT), X-rays, ultrasound imaging, and magnetic resonance imaging (MRI) are utilized for certain diagnoses. In medicinal imaging, CT is the filtering model that uses interesting fields for capturing images in movies. Lung cancer is a type of tumor that results in 1.61 million deceases annually. In Indonesia, lung cancer is rated in 3rd place amongst the predominant tumor [2], for the maximum part, originating in the MIoT center. The earlier detection of lung tumors is not an easy task. About 80% of the people are effectually identified only at the centre or propelled stage of tumor. Lung tumor is placed 10th amongst females and 2nd amongst males worldwide. The data provided in the study is a common depiction of lung tumor position that comprises four fundamental phases [3]. The lung tumor is the 3rd common tumor in women, afterward colorectal and breast tumors. The feature extraction method is the efficient and simplest dimension reduction method in image processing [4]. Classification of subtypes and tumor samples serves high significance in prognosis and diagnosis of dissimilar kinds of tumor. It assists in the accurate forecast of tumor kinds and additionally identifies subtype drug treatment [5]. Several researchers have projected dissimilar classification methods with gene expression information. This method varies from statistical approach to machine learning algorithm for tumor classification [6]. The higher dimension nature of gene expression information makes classification a difficult job, henceforth gene selection is a primary phase in large number of classifications. It assists in enhancing time difficulty and classifier performance by filtering inappropriate features. But, current "feature selection algorithm" suffer from constraint of generalization and scalability; as well, classification created by one FS technique on information mayn't be capable of giving precise result on new dataset [7]. In this situation, Deep Neural Networks (DNN) assist in building scalable and generalized classification and automated feature extraction.

Tran et al. [8] suggest a deep learning (DL) technique to expand classifier efficiency of pulmonary nodules in CT images. This technique employs a 15-layer two-dimensional DL model for automated feature extraction and classifier of pulmonary candidate as nodule or non-nodule. Raj et al. [9] projected the Optimum feature selection (FS) based Medicinal Image Classification with DL technique by integrating classification, preprocessing, and FS. The aim is to derive an optimum FS for efficient medicinal image classifier. To improve the efficiency of the DL method, Opposition-based Crow Search (OCS) approach has been projected.

Asuntha et al. [10] use optimal FS methods namely wavelet transform-based features, HoG, SIFT, Zernike Moment, and local binary patterns (LBP). Afterward extracting geometric, texture, intensity, and volumetric features, Fuzzy Particle swarm optimization (FPSO) approach is employed to select the optimal feature. Lastly, this feature is categorized by the DL method. Kasinathan et al. [11] presented an approach for validating and classifying dissimilar phases of lung cancer development, along with a deep neural system and information gathering with cloud scheme for classifying stages of pulmonary illness. The presented technique projected a Cloud-based Lung Tumor Detector and Stage Classification (Cloud-LTDSC) as a hybrid model for CT images. The presented method firstly designed the active contour system as lung cancer segmentation, and multilayer convolutional neural network (M-CNNs) for categorizing dissimilar phases of lung tumor.

Angeline et al. [12] identify whether cancer existing in the lung is benign, malignant, or unsure with DL concept on datasets lung scans. The severity of a cancer is dependent mainly on the intrinsic ordinal relation of the nodules in the lung at many phases- by phases that are benign, malignant, or unsure. Wang et al. [13] projected a multi-energy level fusion technique using a principal feature enhancement (PFE) block integrating computer science and radiologist knowledge for Nmet forecast.

This article presents a deer hunting optimization with deep convolutional neural network for lung cancer detection and classification (DHODCNN-LCC) model. The proposed DHODCNN-LCC technique initially undergoes pre-processing in two stages namely contrast enhancement and noise removal. Besides, the features extraction process on the pre-processed images takes place using the Nadam optimizer with RefineDet model. In addition, denoising stacked autoencoder (DSAE) model is employed for lung nodule classification. Finally, the DHOA algorithm is utilized for optimal hyper parameter tuning of the DSAE model and thereby results in improved classification performance. The experimental validation of the DHODCNN-LCC technique was implemented against benchmark dataset.

2 The Proposed Model

This article has developed a DHODCNN-LCC model for effective lung cancer detection and classification. The proposed DHODCNN-LCC technique involves a series of subprocesses namely pre-processing, RefineDet based feature extraction, Nadam hyperparameter optimizer, DSAE classification, and DHOA parameter optimization. The DHOA algorithm is utilized for optimal parameter tuning of the DSAE model resulting in improved classifier performance. Fig. 1 demonstrates the overall process of DHODCNN-LCC technique.

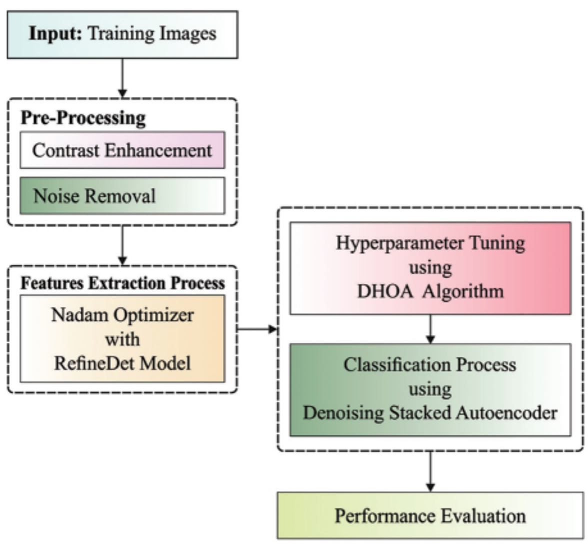

Figure 1: Overall process of DHODCNN-LCC technique

2.1 Pre-processing

At the initial stage, the images are pre-processed in two distinct ways namely adaptive histogram equalization (AHE) based contrast improvement and median filtering (MF) based noise removal. AHE is an image processing approach employed for enhancing the contrast level of the image. It differs from ordinary HE from the respect that adaptive technique calculates many histograms, all equivalent to various sections of images, and utilizes them for redistributing the lightness value of images. It can be appropriate to enhance the local contrast and increase the definition of edges from all the regions of images.

2.2 Feature Extraction Using Optimal RefineDet Model

Next to image pre-processing, the RefineNet model was employed for deriving a useful set of feature vectors. RefineDet [14] is a single stage technique dependent upon the single shot detector (SSD) structure and includes object-detection module (ODM) and anchor-refinement module (ARM). The ARM permits negative hard-refined anchor and positive-refined anchor to ODM that tries to place and classify target object from the input image. The feature in ARM is transmitted to ODM by considering transfer connection block (TCB) that gathers 2 neighbouring feature layers (lower and higher levels) in the ARM as input and executes a deconvolution function to higher level layer for obtaining feature of similar size as lower level layer for generating fusion feature by element-wise summation [15]. The planned TCB offers more contextual data. During the current analysis, it can be utilized RefineDet as baseline method for detecting and classifying images to the subsequent reasons: (1) it can be extremely effectual because of its single stage infrastructure; and (2) it utilizes a refine procedure which simulations "recognition procedure" for determining feasible region. Fig. 2 depicts the RefineNet framework.

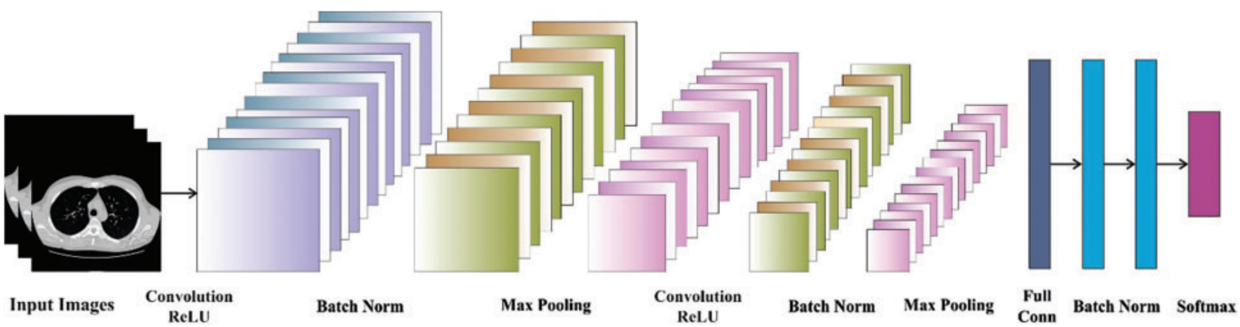

Figure 2: RefineNet structure

To optimally adjust the hyperparameters of the RefineDet model, the Nadam optimizer is applied. Nadam is different from weight update rule [16]. It can be computed as expression of a_r and $\hat{a}$ as illustrated in Eq. (1).

$$\theta_{t+1} = \theta_t - \frac{\eta}{\sqrt{\hat{u}_t + \varepsilon}} \left(\frac{\beta_1 a_{t-1}}{1 - \beta_1^r} + \frac{1 - \beta_1}{1 - \beta_1^t} d_t \right) \tag{1}$$

whereas $\frac{\beta_1 a_{t-1}}{1 - \beta_1^t}$ represents the bias-corrected estimation of momentum vector of the preceding time step. Thus, it is exchanged with $\hat{a}_{t-1}$

$$\theta_{t+1} = \theta_t - \frac{\eta}{\sqrt{\hat{u}_t + \varepsilon}} \left(\beta_1 \hat{a}_{t-1} + \frac{1 - \beta_1}{1 - \beta_1^t} d_t \right) \tag{2}$$

Hence, the Nadam update rule was provided as exchanging bias-corrected estimation of the earlier momentum vector $\hat{a}_{t-1}$ with bias-corrected estimation of present momentum vector $\hat{a}_t$ as illustrated in Eq. (3).

$$\theta_{t+1} = \theta_t - \frac{\eta}{\sqrt{\hat{u}_t + \varepsilon}} \left(\beta_1 \hat{a}_t + \frac{1 - \beta_1}{1 - \beta_1^t} d_t \right) \tag{3}$$

2.3 Image Classification Using DSAE Model

During lung cancer classification, the DSAE model is applied and it allocates proper class labels to it. Denoising Autoencoder (DAE) utilizes the noised input for improving robustness [17]. The noised input $\hat{x}$ has created by arbitrarily adding noise as to primary input x, and the corresponding resultant is $\wedge y \wedge y$. If $\wedge y \wedge y$ reproduces x to highest extent, it represents that auto encoder (AE) is optimum robustness. And L_{DAE} is

$$L_{DAE} = \frac{1}{n} \sum_{i=1}^{n} (x_i - \hat{y}_i)^2 + \frac{\lambda}{2} (\| W_1^2 \|_F^2 + \| W_2^2 \|_F^2) \tag{4}$$

Whereas λ represents the weight constraint for preventing over-fitting. At the same time, it introduces sparsity and noise as to AE that is the SDAE. In Eq. (4), L_{SDAE} is

$$L_{SDAE} = \frac{1}{n} \sum_{i=1}^{n} (x_i - y_i)^2 + \beta \sum_{m=1} KL \left(\rho \| \hat{\rho}_m \right) + \frac{\lambda}{2} (\| W_1^2 \|_F^2 + \| W_2^2 \|_F^2) \tag{5}$$

The DSAE detector was constructed by stacking DAE and training from a greedy layer-wise approach which is the hidden layer of previous AE has been utilized as input of latter one. Generally, the MLNN trained suffer from vanishing gradient problems. If the network weight is upgrading utilizing BP technique, the hidden layer gradient nearby the input is too smaller than upgrade [18]. But, the greedy layer-wise trained adapts 2 phases in fixing the vanishing gradient issues namely top-down supervised fine-tuning and bottom-up unsupervised pre-training. Taking $DSAE_1$ as an instance, their network parameter ω_1, b_1, and f_1 are calculated by the forward propagation. Afterward, f_1 is taken as input of $DSAE_2$ for calculating f_2, and so on still the completion of training. Eventually, every DSAE is stacked for generating a DSAE to more supervised training for implementing the fine-tuning of network weighted.

2.4 Parameter Tuning Using DHOA

Finally, the DHOA algorithm is utilized for optimal parameter tuning of the DSAE model resulting in improved classification performance. A new metaheuristic DHOA approach was projected [19] that is simulated as the hunting of deer by a set of hunters. In order to hunt the deer, the hunter encloses it and moves nearby according to some methods. These methods comprise the consideration of numerous parameters namely the deer position, wind angle, etc. At last, it could obtain the target according to the place of leaders and successors. The main function of this projected approach was demonstrated in Eq. (6).

$$f(x) = max\,(accuracy) \tag{6}$$

The steps to weight optimized utilizing DHO approach. This procedure is demonstrated as:

$$X = \{X_1, X_2, \ldots, X_m\} \ 1 < j \le m \tag{7}$$

Whereas m implies the count of hunters populations (weights). The whole searching space was assumed a circle, thus the wind angle is explained as the circumference of circles. It can be determined as in Eq. (8),

$$\theta_j = 2\pi a \tag{8}$$

In which, the arbitrary number having range of zero and one has demonstrated as a, and the current iteration is defined as J. Next, the position propagation with successor position (X_s) and leader position (X_l) to optimize was recognized. Afterward, the position upgrade method starts with modelling the neighboring efficiency that is demonstrated as in Eq. (9),

$$X_{j+1} = X_l - Y \cdot p \cdot \left| L \times X_l - X_j \right| \tag{9}$$

Whereas, X_j stands for the place at existing iteration and the subsequent iteration place was expressed as X_{j+1}. The 2 co-efficient vectors Z and K are comprised during this approach [20].

$$Z = \frac{1}{4} \log \left(j + \frac{1}{j_{\max}} \right) b \tag{10}$$

$$K = 2 \cdot c \tag{11}$$

In which, the maximal iteration has signified as $j_{\max}$. The parameter b is the values range in -1 to 1, also the value of other parameter c lies from the range of zero and one. An initial place of hunters is demonstrated as $(X, \ Y)$ which gains upgrade based on the location of prey. In the position angle, the place upgrading was executed employing in Eq. (12),

$$X_{j+1} = X_l - p. \left| \cos(v) \times X_l - X_j \right| \tag{12}$$

Whereas, an optimal place was referred to as $B = \phi_{j+1}, X_{b_j}$ and p stands for the arbitrary number. At last, the place upgrade procedure takes place on the fundamental of a successor place before regarding the optimal place. Next, the global search was implemented employing in Eq. (13),

$$X_{j+1} = X_s - Z \cdot p \cdot \left| K \times X_s - X_j \right| \tag{13}$$

The place upgrade method was implemented for identifying an optimum place (i.e., termination condition). Eventually, this optimum solution offers better weight value for DNN, thus, the detection method was executed from an accurate method with minimum error and complexity.

3 Experimental Validation

In this section, the lung cancer classification outcomes of the DHODCNN-LCC model are investigated in detail. The results are inspected using a set of CT images from benchmark dataset [21], which includes 300 images under three classes namely Normal, Benign, and Malignant. A few sample images are demonstrated in Fig. 3.

Fig. 4 demonstrates the confusion matrices of the DHODCNN-LCC model under three runs. The figures portrayed that the DHODCNN-LCC model has resulted in effective classifier results. For instance, in run-1, the DHODCNN-LCC model has classified 92 images under Normal, 96 images under Benign, and 95 images under Malignant. Moreover, in run-2, the DHODCNN-LCC technique has ordered 93 images under Normal, 95 images under Benign, and 98 images under Malignant. Furthermore, in run-3, the DHODCNN-LCC system has classified 91 images under Normal, 95 images under Benign, and 93 images under Malignant.

Tab. 1 provides brief overall classifier outcomes of the DHODCNN-LCC model under three distinct runs.

Figure 3: Sample images

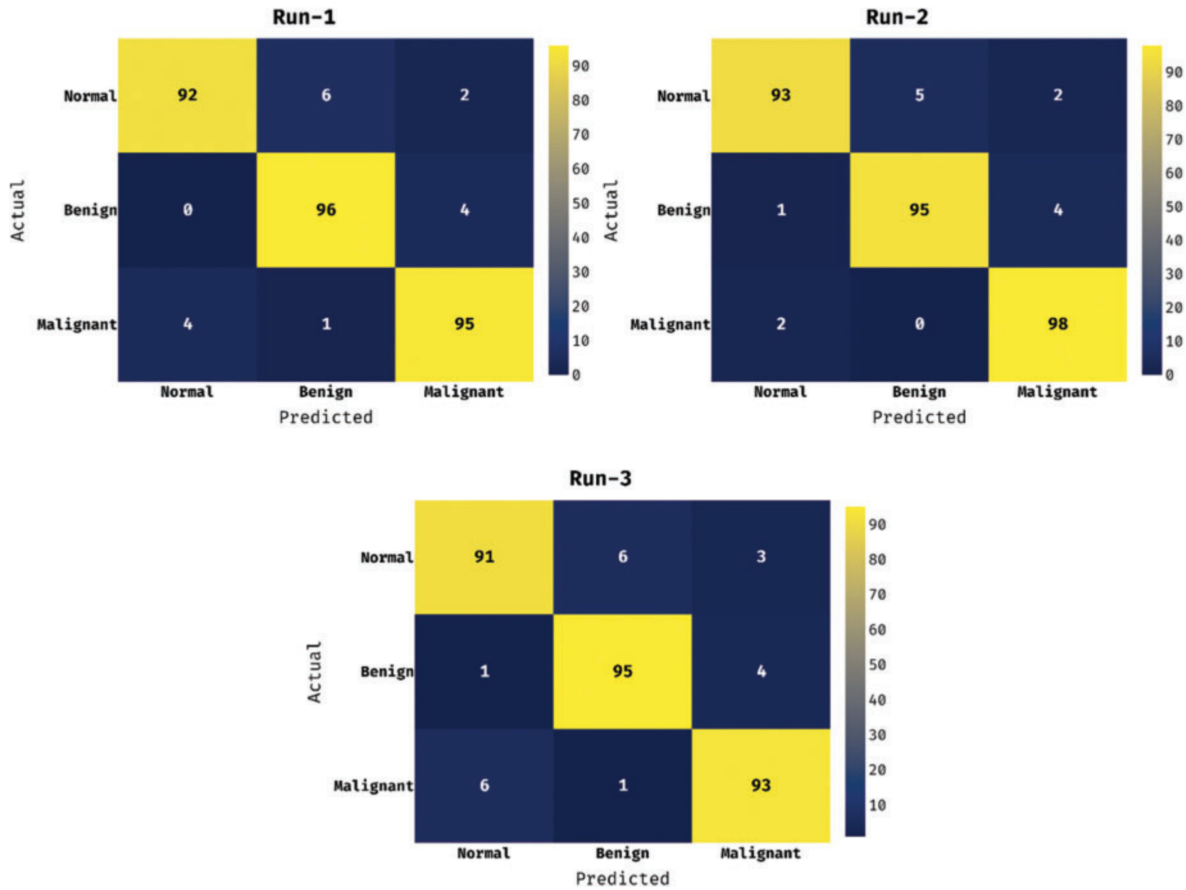

Figure 4: Confusion matrix of DHODCNN-LCC technique with three runs

Table 1: Result analysis of DHODCNN-LCC technique with different classes and runs

Class labels	Accuracy	Sensitivity	Specificity	Precision	Kappa
Run-1					
Normal	96.00	92.00	98.00	95.83	-
Benign	96.33	96.00	96.50	93.20	-
Malignant	96.33	95.00	97.00	94.06	-
Average	96.22	94.33	97.17	94.37	91.50
Run-2					
Normal	96.67	93.00	98.50	96.88	-
Benign	96.67	95.00	97.50	95.00	-
Malignant	97.33	98.00	97.00	94.23	-
Average	96.89	95.33	97.67	95.37	93.00

(Continued)

Table 1: Continued

Class labels	Accuracy	Sensitivity	Specificity	Precision	Kappa
Run-3					
Normal	94.67	91.00	96.50	92.86	-
Benign	96.00	95.00	96.50	93.14	-
Malignant	95.33	93.00	96.50	93.00	-
Average	95.33	93.00	96.50	93.00	89.50

Fig. 5 demonstrates the overall classification results of the DHODCNN-LCC model under run-1. The results indicated that the DHODCNN-LCC model has effectually recognized all three classes. For instance, the DHODCNN-LCC model has identified normal class with $accu_y$, $sens_y$, $spec_y$, and $prec_n$ of 96%, 92%, 98%, and 95.83% correspondingly. Also, the DHODCNN-LCC model has recognized Benign class with $accu_y$, $sens_y$, $spec_y$, and $prec_n$ of 96.33%, 96%, 96.50%, and 93.20% respectively. Along with that, the DHODCNN-LCC model has identified Malignant class with $accu_y$, $sens_y$, $spec_y$, and $prec_n$ of 96.33%, 95%, 97%, and 94.06% respectively.

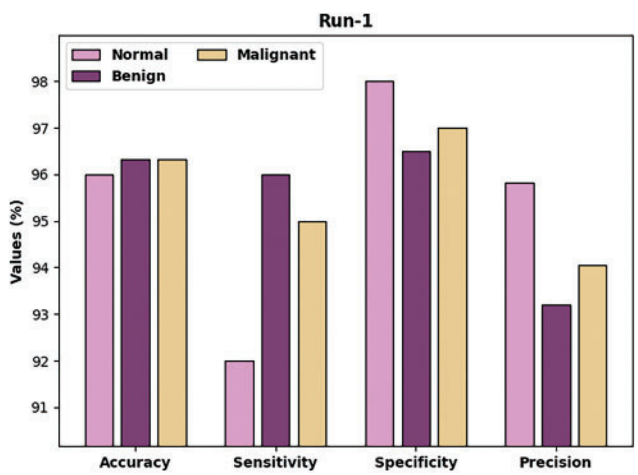

Figure 5: Result analysis of DHODCNN-LCC technique under run-1

Fig. 6 defines the overall classification results of the DHODCNN-LCC approach under run-2. The results indicated that the DHODCNN-LCC model has effectually recognized all three classes. For instance, the DHODCNN-LCC approach has identified normal class with $accu_y$, $sens_y$, $spec_y$, and $prec_n$ of 96.67%, 93%, 98.50%, and 96.88% correspondingly. Similarly, the DHODCNN-LCC model has identified Benign class with $accu_y$, $sens_y$, $spec_y$, and $prec_n$ of 96.67%, 95%, 97.50%, and 95% correspondingly. At last, the DHODCNN-LCC model has identified Malignant class with $accu_y$, $sens_y$, $spec_y$, and $prec_n$ of 97.33%, 98%, 97%, and 94.23% correspondingly.

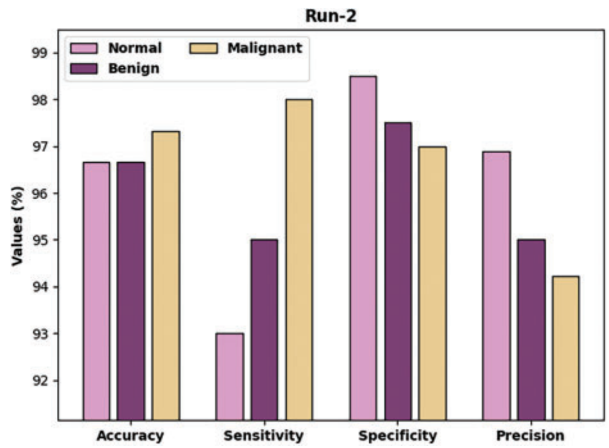

Figure 6: Result analysis of DHODCNN-LCC technique under run-2

Fig. 7 illustrates the overall classification results of the DHODCNN-LCC method under run-3. The outcomes indicated that the DHODCNN-LCC approach has effectually recognized all three classes. For instance, the DHODCNN-LCC model has identified normal class with $accu_y$, $sens_y$, $spec_y$, and $prec_n$ of 94.67%, 91%, 96.50%, and 92.86% correspondingly. In addition, the DHODCNN-LCC approach has identified Benign class with $accu_y$, $sens_y$, $spec_y$, and $prec_n$ of 96%, 95%, 96.50%, and 93.14% respectively. Finally, the DHODCNN-LCC methodology has identified Malignant class with $accu_y$, $sens_y$, $spec_y$, and $prec_n$ of 95.33%, 93%, 96.50%, and 93% correspondingly.

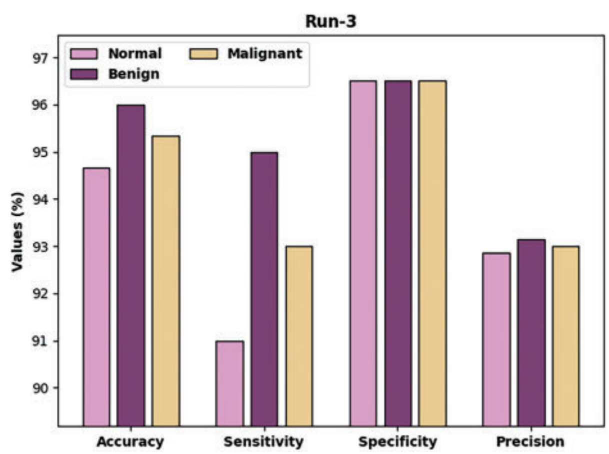

Figure 7: Result analysis of DHODCNN-LCC technique under run-3

Tab. 2 and Fig. 8 examine the overall result analysis of DHODCNN-LCC technique with different measures. The results indicated that the DHODCNN-LCC model has effectually identified all three runs. For instance, with run-1, the DHODCNN-LCC technique has obtained results with $accu_y$, $sens_y$, $spec_y$, $prec_n$, and kappa of 96.22%, 94.33%, 97.17%, 94.37%, and 91.50% respectively. Likewise, with run-2, the DHODCNN-LCC approach has obtained results with $accu_y$, $sens_y$, $spec_y$, $prec_n$, and kappa of 96.89%, 95.33%, 97.67%, 95.37%, and 93% correspondingly. Finally, with run-3, the DHODCNN-LCC technique has achieved results with $accu_y$, $sens_y$, $spec_y$, $prec_n$, and kappa of 95.33%, 93%, 96.50%, 93%, and 89.50% respectively.

Table 2: Overall result analysis of DHODCNN-LCC technique with different measures

No. of runs	Accuracy	Sensitivity	Specificity	Precision	Kappa
Run-1	96.22	94.33	97.17	94.37	91.50
Run-2	96.89	95.33	97.67	95.37	93.00
Run-3	95.33	93.00	96.50	93.00	89.50

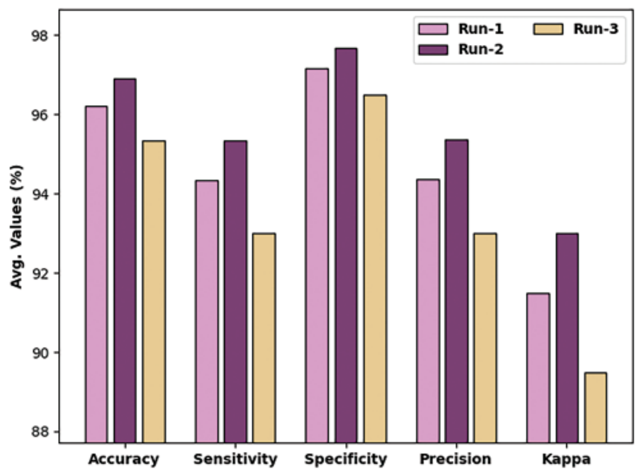

Figure 8: Overall result analysis of DHODCNN-LCC technique with different measures

For demonstrating the enhanced performance of the DHODCNN-LCC model, a comparison study is made in Tab. 3 [22] with existing models namely radial basis function (RBF), artificial neural network (ANN), k-nearest neighbor (KNN), deep neural network (DNN), and optimal deep neural network (ODNN). Fig. 9 examines the $sens_y$ and $spec_y$ investigation of the DHODCNN-LCC model with recent models. The experimental results indicated that the RBF model has obtained worse results with least values of $sens_y$ and $spec_y$. Concurrently, the DNN approach has shown somewhat improved values of $sens_y$ and $spec_y$. Followed by, the ANN and KNN models have resulted in moderately closer values of $sens_y$ and $spec_y$. Afterward, the ODNN model has accomplished reasonable value of $sens_y$ and $spec_y$. However, the DHODCNN-LCC model has resulted in maximum $sens_y$ and $spec_y$ of 95.33% and 97.67% respectively.

Table 3: Comparative analysis of DHODCNN-LCC algorithm with recent approaches

Methods	Accuracy	Sensitivity	Specificity	Precision	Kappa
RBF model	83.72	90.89	46.49	90.44	87.38
ANN model	86.27	90.97	80.78	68.80	81.62
KNN model	90.19	92.33	88.43	85.49	69.35
DNN model	91.93	83.41	94.92	88.08	90.17
ODNN model	94.04	92.31	89.31	85.59	90.54
DHODCNN-LCC	96.89	95.33	97.67	95.37	93.00

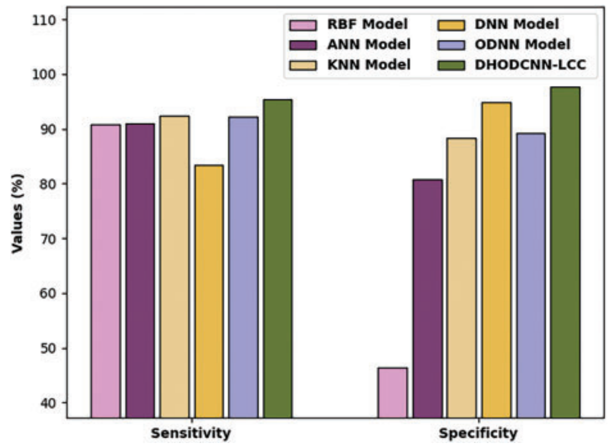

Figure 9: $Sens_y$ and $Spec_y$ analysis of DHODCNN-LCC technique with recent approaches

Fig. 10 examines the acc_y, $prec_n$, and kappa investigation of the DHODCNN-LCC model with recent models. The experimental results indicated that the RBF system has obtained worse results with least values of acc_y, $prec_n$, and kappa. Besides, the DNN technique has shown somewhat improved values of acc_y, $prec_n$, and kappa. Followed by, the ANN and KNN approaches have resulted in moderately closer values of acc_y, $prec_n$, and kappa. Likewise, the ODNN algorithm has accomplished reasonable value of acc_y, $prec_n$, and kappa. At last, the DHODCNN-LCC model has resulted in maximum acc_y, $prec_n$, and kappa of 96.89%, 95.37%, and 93% correspondingly.

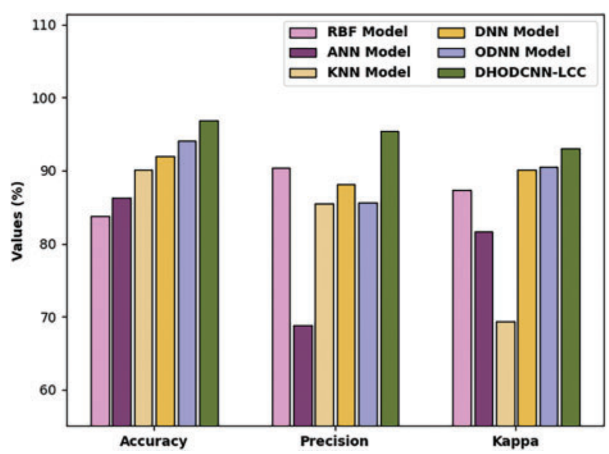

Figure 10: Comparative analysis of DHODCNN-LCC technique with recent approaches

After examining the results and discussion, it is ensured that the DHODCNN-LCC model has outperformed other methods under all aspects.

4 Conclusion

This article has developed a DHODCNN-LCC model for effective lung cancer detection and classification. The proposed DHODCNN-LCC technique involves a series of subprocesses namely pre-processing, RefineDet based feature extraction, Nadam hyperparameter optimizer, DSAE classification, and DHOA parameter optimization. The DHOA algorithm is utilized for optimal parameter tuning of the DSAE model resulting in improved classification performance. The experimental validation of the DHODCNN-LCC technique was implemented against benchmark dataset and the outcomes are assessed under different aspects. The experimental outcomes reported the superior outcomes of the DHODCNN-LCC technique over the recent approaches in terms of different measures. Therefore, the DHODCNN-LCC approach was employed as an effectual tool for lung cancer classification. In future, image segmentation techniques are included to improve the classification performance.

Acknowledgement: This project was funded by the Deanship of Scientific Research (DSR), King Abdulaziz University, Jeddah, Under Grant No. (D-782-980-1443). The authors, therefore, gratefully acknowledge DSR technical and financial support.

Funding Statement: This work was funded by the Deanship of Scientific Research (DSR), King Abdulaziz University, Jeddah, Under Grant No. (D-782-980-1443).

Conflicts of Interest: The authors declare that they have no conflicts of interest to report regarding the present study.

References

[1] R. Tekade and K. Rajeswari, "Lung cancer detection and classification using deep learning," in *2018 Fourth Int. Conf. on Computing Communication Control and Automation (ICCUBEA)*, Pune, India, pp. 1–5, 2018.

[2] J. Alam, S. Alam and A. Hossan, "Multi-stage lung cancer detection and prediction using multi-class svm classifier," in *2018 Int. Conf. on Computer, Communication, Chemical, Material and Electronic Engineering (IC4ME2)*, Rajshahi, Bangladesh, pp. 1–4, 2018.

[3] S. Thakur, D. Singh and J. Choudhary, "Lung cancer identification: A review on detection and classification," *Cancer and Metastasis Reviews*, vol. 39, no. 3, pp. 989–998, 2020.

[4] W. Abdul, "An automatic lung cancer detection and classification (alcdc) system using convolutional neural network," in *2020 13th Int. Conf. on Developments in eSystems Engineering (DeSE)*, Liverpool, United Kingdom, pp. 443–446, 2020.

[5] N. Nasrullah, J. Sang, M. S. Alam and H. Xiang, "Automated detection and classification for early stage lung cancer on CT images using deep learning," in *Proc. Society of Photo-Optical Instrumentation Engineers (SPIE), Pattern Recognition and Tracking XXX*, vol. 10995, Baltimore, United States, pp. 27, 2019.

[6] F. Taher, N. Werghi and H. Al-Ahmad, "Rule based classification of sputum images for early lung cancer detection," in *2015 IEEE Int. Conf. on Electronics, Circuits, and Systems (ICECS)*, Cairo, Egypt, pp. 29–32, 2015.

[7] W. Alakwaa, M. Nassef and A. Badr, "Lung cancer detection and classification with 3d convolutional neural network (3D-CNN)," *International Journal of Advanced Computer Science and Applications*, vol. 8, no. 8, pp. 409–417, 2017.

[8] G. S. Tran, T. P. Nghiem, V. T. Nguyen, C. M. Luong and J. C. Burie, "Improving accuracy of lung nodule classification using deep learning with focal loss," *Journal of Healthcare Engineering*, vol. 2019, pp. 1–9, 2019.

[9] R. J. S. Raj, S. J. Shobana, I. V. Pustokhina, D. A. Pustokhin, D. Gupta *et al.,* "Optimal feature selection-based medical image classification using deep learning model in internet of medical things," *IEEE Access*, vol. 8, pp. 58006–58017, 2020.

[10] A. Asuntha and A. Srinivasan, "Deep learning for lung cancer detection and classification," *Multimedia Tools and Applications*, vol. 79, no. 11–12, pp. 7731–7762, 2020.

[11] G. Kasinathan and S. Jayakumar, "Cloud-based lung tumor detection and stage classification using deep learning techniques," *BioMed Research International*, vol. 2022, pp. 1–17, 2022.

[12] R. Angeline, S. N. Kanna, N. G. Menon and B. Ashwath, "Identifying malignancy of lung cancer using deep learning concepts," in *Artificial Intelligence in Healthcare, Advanced Technologies and Societal Change Book Series (ATSC)*, Singapore: Springer, pp. 35–46, 2022.

[13] Y. W., Wang, C. J. Chen, T. C. Wang, H. C. Huang, H. M. Chen *et al.,* "Multi-energy level fusion for nodal metastasis classification of primary lung tumor on dual energy CT using deep learning," *Computers in Biology and Medicine*, vol. 141, pp. 105185, 2022.

[14] S. Zhang, L. Wen, X. Bian, Z. Lei and S. Z. Li, "Single-shot refinement neural network for object detection," in *Proc. of the IEEE Conf. on Computer Vision and Pattern Recognition*, Salt Lake City, UT, USA, pp. 4203–4212, 2018.

[15] C. Sun, Y. Ai, S. Wang and W. Zhang, "Dense-refinedet for traffic sign detection and classification," *Sensors*, vol. 20, no. 22, pp. 6570, 2020.

[16] S. Bera and V. K. Shrivastava, "Analysis of various optimizers on deep convolutional neural network model in the application of hyperspectral remote sensing image classification," *International Journal of Remote Sensing*, vol. 41, no. 7, pp. 2664–2683, 2020.

[17] Y. Huang and Q. Xu, "Electricity theft detection based on stacked sparse denoising autoencoder," *International Journal of Electrical Power & Energy Systems*, vol. 125, pp. 106448, 2021.

[18] P. Vincent, H. Larochelle, Y. Bengio and P. A. Manzagol, "Extracting and composing robust features with denoising autoencoders," in *Proc. of the 25th International Conf. on Machine Learning-ICML '08*, Helsinki, Finland, pp. 1096–1103, 2008.

[19] G. Brammya, S. Praveena, N. N. Preetha, R. Ramya, B. Rajakumar *et al.,* "Deer hunting optimization algorithm: A new nature-inspired meta-heuristic paradigm," *The Computer Journal*, 2019, https://doi.org/10.1093/comjnl/bxy133.

[20] G. Agarwal and H. Om, "Performance of deer hunting optimization based deep learning algorithm for speech emotion recognition," *Multimedia Tools and Applications*, vol. 80, no. 7, pp. 9961–9992, 2021.

[21] 2003. http://www.via.cornell.edu/lungdb.html.

[22] S. K. Lakshmanaprabu, S. N. Mohanty, K. Shankar, N. Arunkumar and G. Ramirez, "Optimal deep learning model for classification of lung cancer on CT images," *Future Generation Computer Systems*, vol. 92, pp. 374–382, 2019.